Environmental Fluid Mechanics **3:** 55–77, 2003.

A Parameterization of the Roughness Length for the Air-Sea Interface in Free Convection

K. ABDELLA[a,*] and S.J.D. D'ALESSIO[b,**]
[a]*Department of Mathematics, Trent University, Peterborough, Ontario, K9J 7B8, Canada;*
[b]*Department of Applied Mathematics, University of Waterloo, Waterloo, Ontario, N2L 3G1, Canada*

Received 10 August 2001; accepted in revised form 8 August 2002

Abstract. The response of the upper ocean to the parameterization of the roughness length z_0 on the air side of the air-sea interface is studied using a one-dimensional mixed-layer model. In particular, it is shown that in the free convection limit when both the wind speed and the friction velocity approach zero, the familiar Charnock formula for the momentum roughness, which relies solely on wind generation, can be modified to account for contributions arising from the thermally generated turbulence. Therefore, a new parameterization is proposed for the momentum roughness length which extends the Charnock formula down to zero friction velocity. The value of a parameter which enters in the new formulation is determined by making use of exsisting free convection surface flux parameterizations. The effect of the new parameterization on the model performance is tested using data from the ocean weathership station Papa (OWS P), and data from the Long-Term Upper-Ocean Study (LOTUS) experiment. Simulations were carried out using a recently developed one-dimensional, second-order, turbulence closure scheme over diurnal as well as seasonal time scales. The findings suggest that the new momentum roughness parameterization improves the overall agreement between the observed and simulated sea-surface temperature (SST).

1. Introduction

In recent years, there has been increasing interest in the parameterization of the air-sea interface fluxes under free convection conditions [1–3]. In particular, the work of Miller *et al.* [2] demonstrated that the proper representation of fluxes in free convection conditions over the tropical ocean such as in the warm pool region where the wind speed is relatively low is crucial in determining the correct tropical atmosphere-ocean circulation.

These fluxes are typically determined by applying the Monin–Obukhov similarity theory in the surface layer above the roughness sub-layer underneath. The similarity theory is strongly dependent upon the surface roughness and, therefore, the roughness length is required in order to calculate the fluxes. Over a water surface the roughness length is commonly determined using Charnock's formula which is based upon the assumption that, at high winds, the roughness is mainly

*Currently at the American University of Sharjah, P.O. Box 26666, Sharjah, UAE, E-mail: kabdella@dachi.trentu.ca
**E-mail: sdalessio@math.uwaterloo.ca

due to the shorter surface waves and, thus, the roughness length is proportional to the wind stress which produces and supports these waves.

However, under free convection conditions, both the wind speed and the friction velocity approach zero and Charnock's formula is no longer appropriate. The modification of Charnock's formula for a non-rough sea surface of Smith [4] is also inadequate since it becomes singular in the limit of zero friction velocity. In this study we propose a new roughness length formula for z_0 on the air side of the air-sea interface by making use of the logarithmic profile to relate the free convection velocity to the friction velocity and employing the concept of an internal boundary layer. The new parameterization reduces to the usual Charnock formula in scenarios where strong winds exist, but also accounts for contributions from thermally generated turbulence in the limit of free convection and can be applied right down to zero friction velocity.

The effect of the new parameterization is investigated using an oceanic one-dimensional, second-order, turbulence model driven by a non-iterative surface flux scheme [5, 6]. The simulation is compared against the data set from ocean weathership station Papa (OWS P) and data from the LOTUS experiment. The results obtained suggest that the new parameterization is physically plausible.

The paper is organized as follows. In Section 2 we provide a brief description of the surface flux and roughness length parameterizations as well as a discussion of the existing approaches dealing with free convection cases. In Section 3 we present the proposed new formulation and derive the value of a parameter appearing in the formula. Then, in Section 4, we analyze the sensitivity of the mixed-layer model to the new parameterization by comparing model simulations against the observational data. Finally, we present our conclusions and possible extensions of this work in Section 5.

2. Surface Flux Parameterization

The vertical fluxes of momentum, sensible heat and moisture and other characteristics of turbulence in the atmospheric surface layer are well described by the Monin–Obukhov (1954) similarity theory [7]. The Monin–Obukhov theory states that, under stationary and horizontally homogeneous conditions, the atmospheric surface layer fluxes are uniform functions of the Monin–Obukhov stability parameter

$$\xi(z) = \frac{z}{L}, \tag{1}$$

where z is the vertical height and L is the Monin–Obukhov length given by

$$L = \frac{T_0 u_*^2}{kg\theta_*} . \tag{2}$$

Here, g is the acceleration due to gravity, T_0 is some representative air temperature (in Kelvin), k is the von Karman constant (assumed to be 0.4 in this study), u_* is the atmospheric friction velocity, and θ_* is the atmospheric temperature scale given by

$$\theta_* = -\frac{H_0}{u_*}, \tag{3}$$

where

$$H_0 = \left(\overline{w'\theta_v'}\right)_0 = -u_*(\theta_* + 0.61\overline{\theta_0}q_*), \tag{4}$$

is the surface heat flux with q_* denoting the humidity scale. The Monin–Obukhov stability parameter ξ, is positive when the atmospheric surface layer is convectively stable, negative when it is unstable and zero when it is neutral. According to the Monin–Obukhov theory, the mean wind (taken for convenience to be in the x direction), temperature and humidity in the atmospheric surface layer can be written in the form

$$\frac{kz}{u_*}\frac{\partial\overline{U}}{\partial z} = \phi_m(\frac{z}{L}), \tag{5}$$

$$\frac{kz}{\theta_*}\frac{\partial\overline{\theta}}{\partial z} = \phi_h(\frac{z}{L}), \tag{6}$$

$$\frac{kz}{q_*}\frac{\partial\overline{q}}{\partial z} = \phi_q(\frac{z}{L}), \tag{7}$$

where ϕ_m, ϕ_h, ϕ_q are universal similarity functions which depend only upon the stability parameter ξ and relate the fluxes to the gradients. The empirical determination of these functions has been the focus of extensive micrometeorological experiments. With the functions ϕ_m, ϕ_h, ϕ_q known, the above equations can be integrated to obtain the mean profiles $\overline{U}(z)$, $\overline{\theta}(z)$, $\overline{q}(z)$. The integration procedure introduces the constants z_0, z_t and z_q which appear in the expressions for $\overline{U}(z)$, $\overline{\theta}(z)$ and $\overline{q}(z)$ respectively. These constants are known as roughness lengths; z_0 is the momentum roughness defined as the height where the mean wind speed vanishes while z_t and z_q are the heat and moisture roughness respectively denoting the heights where $\overline{\theta}$ and $\overline{q}$ assume the corresponding surface values. In general, the lengths z_0, z_t and z_q will be different and will depend upon the surface geometry.

Integrating Equations (5–7) with respect to z from the relevant roughness height to the reference height z_1 one obtains the following relationships between the scaling parameters (u_*, θ_* and q_*) and the mean profiles,

$$u_* = \frac{k\overline{U_1}}{\ln(\frac{z_1}{z_0}) - \psi_m(\frac{z_1}{L}) + \psi_m(\frac{z_0}{L})}, \tag{8}$$

$$\theta_* = \frac{kPr^{-1}(\overline{\theta_1} - \overline{\theta_0})}{\ln(\frac{z_1}{z_t}) - \psi_h(\frac{z_1}{L}) + \psi_h(\frac{z_t}{L})}, \tag{9}$$

$$q_* = \frac{kPr^{-1}(\overline{q_1} - \overline{q_0})}{\ln(\frac{z_1}{z_q}) - \psi_q(\frac{z_1}{L}) + \psi_q(\frac{z_q}{L})}. \tag{10}$$

Here, ψ_m, ψ_h and ψ_q represent the integrated flux-profile relationships for momentum, heat and moisture respectively, Pr is the neutral turbulent Prandtl number, $\overline{U_1}, \overline{\theta_1}, \overline{q_1}$ are the mean profiles evaluated at $z = z_1$ and $\overline{\theta_0}, \overline{q_0}$ are the mean profiles evaluated at the surface. Once u_*, θ_* and q_* are determined, the surface fluxes of momentum $\tau = \sqrt{\tau_x^2 + \tau_y^2}$, sensible heat Q_s, and latent heat Q_e, which are needed to drive the mixed layer, can then be computed using the relations

$$\tau = \rho_a u_*^2, \tag{11}$$

$$Q_s = -\rho_a c_{pa} u_* \theta_*, \tag{12}$$

$$Q_e = -\lambda \rho_a u_* q_*, \tag{13}$$

where ρ_a, c_{pa} are the density and specific heat of air respectively, and λ is the latent heat of vaporization.

According to the flux profile relationships of Businger *et al.* [8], the following integrated flux relationships were proposed by Paulson [9] and Dyer [10] for unstable conditions ($L < 0$):

$$\psi_m = 2\ln\left(\frac{1+\overline{x}}{2}\right) + \ln\left(\frac{1+\overline{x}^2}{2}\right) - 2\tan^{-1}(\overline{x}) + \frac{\pi}{2}, \tag{14}$$

$$\psi_h = \psi_q = 2\ln\left(\frac{1+\overline{x}^2}{2}\right) . \tag{15}$$

where $\overline{x} = (1 - 16\xi)^{1/4}$ and $\xi = z_1/L$, while

$$\psi_m = Pr\psi_h = Pr\psi_q = -4.7\xi, \tag{16}$$

for stable conditions ($L > 0$). However, under very stable conditions Beljaars and Holtslag [11] demonstrated that the linear flux-profile relationship of Equation (16) leads to strongly suppressed turbulence and proposed the following alternative formulations for stable conditions

$$-\psi_m = a\xi + b\left(\xi - \frac{c}{d}\right)\exp(-d\xi) + \frac{bc}{d}, \tag{17}$$

$$-\psi_h = -\psi_q = \left(1 + \frac{2}{3}a\xi\right)^{\frac{3}{2}} + b\left(\xi - \frac{c}{d}\right)\exp(-d\xi) + \frac{bc}{d} - 1, \tag{18}$$

where $a = 1.0$, $b = 0.667$, $c = 5$ and $d = 0.35$.

For a given roughness, mean profiles and reference height, Equations (2) and (8–10) constitute an algebraic system of four equations in the four unknowns u_*, θ_*, q_* and ξ. However, since the system is highly nonlinear, its solution generally involves costly iterative procedures. Recognizing this difficulty, a number of non-iterative approximate solutions have been proposed over the past few decades [6] (hereafter AM96) [12]). In this study, we consider the the non-iterative surface flux formulation of AM96 which is based upon an asymptotic approximation. This scheme is currently used in the Canadian Centre for Climate Modelling and Analysis General Circulation Model (GCM). A brief description of this formulation is provided in Appendix A.

In order to compute the surface fluxes using any of the above or other formulations, one needs to obtain an appropriate value of the roughness parameters. Over the ocean surface, the momentum roughness is typically parameterized using the Charnock [13, 14] formula given by

$$z_0 = \frac{\alpha}{g} u_*^2 \tag{19}$$

where the Charnock constant α typically ranges from 0.014 [13, 14] to 0.018 [16]. In our study $\alpha = 0.015$ is used. The Charnock relation is based on dimensional considerations and the assumption, that at high winds, the roughness of the sea surface is due mainly to the mean square surface displacement of the short gravity waves. Since the relation does not take the sea state into account, the constant α in a coupled atmosphere-ocean system can be modified to better reflect the sea state. This is usually done by expressing α as a function of the wave-induced stress [17] or the wave age [18]. For moderate winds, Monin and Yaglom [19] proposed that the momentum roughness could be determined by the scale of the molecular sublayer which led to the following alternate formulation suggested by Smith [4]:

$$z_0 = \frac{\alpha}{g} u_*^2 + r \frac{\nu}{u_*}, \tag{20}$$

where $\nu = 0.000014 m^2/s$ is the viscosity of air and $r = 0.11$.

2.1. FREE CONVECTION LIMIT

The proper representation of surface fluxes in free convective conditions over the ocean surface such as in the warm-pool region is important to atmospheric circulation models because this determines in part how well the atmosphere-ocean coupling within a model responds to sea-surface temperature anomalies [2].

In the limit of free convection, both the mean wind speed and the friction velocity u_* approach zero. In this case, the traditional Monin–Obukhov theory becomes singular. Moreover, while the Charnock's formula leads to zero roughness, Smith's modified formulation for the momentum roughness becomes singular.

Based on the idea that free convection can be treated as a special case of forced convection in which the near surface forcing wind is produced by the gusts that are driven by the large eddies in the convective mixed layer, Sykes *et al.* [20] developed a scaling analysis for the free convective limit. In this approach the gustiness effect is included by replacing the near surface wind $\overline{U_s}$ by $\overline{U}_{s1}$ which is given by,

$$\overline{U}_{s1} = \sqrt{\overline{U_s}^2 + (\beta w_*)^2}, \tag{21}$$

where the parameter β is of the order of unity and w_* is the Deardorff free convection velocity scale given by

$$w_* = \left(\frac{g}{T_0} H_0 z_i\right)^{\frac{1}{3}}, \tag{22}$$

where z_i is the height of the atmospheric boundary layer.

Beljaars [1] demonstrated that, provided that the modified near surface wind is used, the Monin–Obukhov theory continues to be valid in the free convection limit. This idea was later used by AM96 to develop a non-iterative surface flux parameterization for the free convection limit.

In this paper we consider the momentum roughness singularity that exists over the ocean in this limit. In the next section we propose a modification to the Charnock formula to eliminate this difficulty.

3. Proposed Surface Roughness to Account for Free Convection

As described above, Charnock's formula unrealistically underestimates the value of the momentum roughness in the free convection limit while Smith's formulation leads to a singularity in the limit of zero friction velocity. Therefore, we propose the following formulation given by

$$z_0 = \frac{\alpha}{g}(u_*^2 + \gamma w_*^2), \tag{23}$$

where γ is a parameter that needs to be determined. This extension is analogous to Equation (20) and implies that the surface roughness is composed of two positive contributions resulting from mechanically generated (wind-induced) and thermally generated (heat-induced) turbulence.

In cases of moderate to strong winds the u_* term in Equation (23) dominates and the expression essentially becomes the classic Charnock formula. However, at low enough wind speeds, the u_* term becomes negligible and the w_* term becomes dominant leading to the new formulation for z_0 in the free convection limit

$$z_{0fc} = \frac{\alpha\gamma}{g} w_*^2, \tag{24}$$

where z_{0fc} denotes the momentum roughness in the free convection limit. Therefore, this new formulation extends Charnock's formula down to zero friction velocity and removes the singularity of Smith's formula by accounting for the surface roughness due to free convective transfers. In the following section we shall describe how the value of γ is determined using this limiting case. The term z_{0fc} can be thought of as a correction term to the Charnock formula. In most cases (i.e., moderate to strong winds) this correction will be of little consequence and this is reflected in the value of γ which is discussed next.

3.1. DETERMINATION OF γ

The basic methodology adopted to determine the parameter γ is to apply the formula (23) for z_0 in the limit of free convection in the atmospheric surface layer and to make use of the well established similarity theory which is known to be valid.

Following the free convection description of Sykes *et al.* [20], we define z_s as the inner depth over which the surface effects blend into the average free convection boundary layer. Neglecting both molecular and stability effects, the wind speed increases logarithmically so that z_s can be obtained by matching the logarithmic velocity profile with the modified free-convection gustiness velocity βw_* and therfore satisfies

$$\frac{u_*}{k} \ln(\frac{z_s}{z_0}) = \beta w_* \ . \tag{25}$$

From this it follows that

$$z_0 = z_s \exp(-\beta k w_*/u_*) \ . \tag{26}$$

Using a similar argument for the temperature we obtain

$$\Delta\theta = Pr \frac{H_0}{ku_*} \ln(\frac{z_s}{z_0}), \tag{27}$$

where $\Delta\theta = \overline{\theta}_s - \overline{\theta}_m$ is the difference between the surface temperature, $\overline{\theta}_s$, and the atmospheric mixed layer temperature, $\overline{\theta}_m$, at the top of the inner layer z_s. Therefore, eliminating the logarithmic term using Equation (25) we obtain

$$u_*^2 = \frac{Pr\beta H_0 w_*}{\Delta\theta} \ . \tag{28}$$

While the large eddies in the mixed layer are on the scale of the boundary layer height z_i, the small eddies in the surface layer vary on the scale of the inner depth z_s. Therefore, a scaling analysis on the balance of the horizontal momentum equation [20] yields

$$\frac{u_*^2}{z_s} = \beta_1 \frac{w_*^2}{z_i}, \tag{29}$$

where β_1 is a dimensionless parameter. Hence, using equation (28) for u_* and using Equation (22) for w_* gives

$$z_s = \frac{\beta_2 T_0 w_*^2}{g\Delta\theta} \ , \tag{30}$$

where $\beta_2 = \beta Pr/\beta_1$.

Combining (26) and (30) we obtain the result

$$z_0 = \frac{C_0}{g} w_*^2, \tag{31}$$

where $C_0 = \beta_2 \dfrac{T_0}{\Delta\theta} \exp(-\beta k w_*/u_*)$. Now, by definition of the Monin–Obukhov length, L, and by Equation (22) we obtain the relation

$$H_0 = -\frac{T_0 u_*^3}{kgL} = \frac{T_0 w_{*a}^3}{g z_i}, \tag{32}$$

from which it follows that

$$\frac{w_*}{u_*} = (-\frac{z_i}{kL})^{1/3} \tag{33}$$

and therefore

$$C_0 = \frac{\beta_2 T_0}{\Delta\theta} \exp(-\beta k (-\frac{z_i}{kL})^{1/3}) \ . \tag{34}$$

From Abdella and McFarlane [6], the quantity $\beta k(-z_i/kL)^{1/3}$ under conditions of free convection can be approximated as

$$\beta k(-\frac{z_i}{kL})^{1/3} \approx \frac{\beta^{1/3} k}{Pr^{1/3} b_h^{2/9} C_{MN}^{1/6} f_c^{1/9}} \tag{35}$$

where f_c is a free convection correction parameter, C_{MN} is the transfer coefficient for momentum in neutral conditions and b_h is a nondimensional coefficient which depends upon the stability.

Using the typical values $f_c = 2.1$, $k = 0.4$, $\beta = 1.2$, $Pr = 0.74$,$b_h = 1.2 \times 10^{-4}$,$C_{MN} = 9 \times 10^{-4}$, $\beta_1 = 2.0$ and $T_0 = 300K$ [1, 6, 20, 21] we find that $C_0 = 0.004/\Delta\theta$. Thus, in the free convection limit

$$z_0 = \frac{C_0}{g} w_*^2 = \frac{\alpha\gamma}{g} w_*^2 \tag{36}$$

and substituting $\alpha = 0.015$ for the Charnock constant we finally arrive at the result

$$\gamma = \frac{0.27}{\Delta\theta} \ . \tag{37}$$

Note that the value of γ can easily be modified to take the sea state into account. In this case we obtain $\gamma = C_0/\alpha$ where α can be expressed either in terms of the wave-induced stress [17] or wave age [18]. Further, to take wave breaking into account Craig and Banner [22] suggest using $\alpha \approx 1400$. Clearly, when $\Delta\theta \leq 0$, equation (36) is meaningless. However, $\Delta\theta = 0$ corresponds to neutral stability while $\Delta\theta < 0$ reflects a stable atmospheric boundary layer. Therefore, $\Delta\theta \leq 0$

implies that $w_* = 0$ and consequently Equation (23) reduces to the usual Charnock formula. In practice, the term $\alpha\gamma w_*^2/g$ in Equation (23) will only become significant when $\Delta\theta > 1°C$ since otherwise z_0 will be dominated by the term $\alpha u_*^2/g$. Furthermore, based on the OWS P and LOTUS data sets, one finds that $\Delta\theta$ is empirically bounded by $|\Delta\theta| < 3°C$. Knowing this enables us to eliminate the dependence of $\Delta\theta$ by averaging γ over the interval $1°C < \Delta\theta < 3°C$ where Equation (23) is expected to be valid. This leads to the value $\gamma \approx 0.15$ as a reliable estimate, and makes the parameterization for z_0 both more practical and simpler to implement. The numerical value of γ reinforces the idea that z_{0fc} represents a small correction to the widely used Charnock formula. This correction will be an order of magnitude smaller than the Charnock result when u_* and w_* are of comparable size. It is only when $u_* \sim 0$ that z_{0fc} plays an important role.

4. Numerical Simulations and Analysis

We next present the numerical results produced by the mixed-layer model. Meteorological data sets from OWS P and LOTUS were used to provide the atmospheric conditions that will drive the model. The surface fluxes resulting from the data sets are computed using the AM96 surface flux algorithm previously mentioned in conjunction with the new parameterization for the roughness length.

The mixed-layer model employed in this study is the second-order, turbulence closure scheme of D'Alessio *et al.* [5]. This mixed-layer model can be classified as a Mellor-Yamada [23, 24] type model. The differences and details of the model are fully explained in D'Alessio *et al.* [5].

One-dimensional mixed-layer models generally ignore the effects of horizontal advection and the role of the deeper ocean. In order to assess the validity of these assumptions the heat balance can be checked over the simulation periods. If the temperature $\overline{\theta}$ is integrated throughout the water column from $z = -D$ to the surface $z = 0$ and then integrated again in time, a typical mixed-layer model would predict the following balance:

$$\int_{-D}^{0} \overline{\theta}(t)dz - \int_{-D}^{0} \overline{\theta}(t=0)dz = \frac{1}{\rho_0 c_p}\int_0^t (I_0 + Q)d\overline{t}\ . \tag{38}$$

Here, D represents a sufficiently large depth whereby the surface fluxes become insignificant, I_0 is the transmitted solar radiation at the surface, Q is the total heat received by the ocean at the surface, c_p is the specific heat of water and ρ_0 is a reference water density. The left-hand side (LHS) of Equation (38) represents changes in the vertical heat content which can be computed from both observed temperature profiles as well as from simulated temperature profiles. The right-hand side (RHS) of Equation (38) refers to time-integrated surface fluxes of heat which can be computed in part using the surface flux algorithm. A similar expression describing the vertical salt and momentum content can also be derived; however, since observed salinity data are not available and velocity measurements are either absent or unreliable, this will not be considered. Equation (38) basically checks if the changes in temperature profiles are consistent with the time-integrated surface fluxes. If not, then there must be processes responsible for this imbalance and since these processes are not taken into account in the model, the one-dimensional mixed-layer model is not valid over that simulation period. For the LOTUS data set a comparison between the LHS and RHS of Equation (38) is in order since I_0 was recorded. Such a comparison at OWS P would not be appropriate since I_0 was not measured. The parameterization of I_0 would introduce additional errors which would make it difficult to assess the validity of a one-dimensional model.

The model was driven by observational data spanning both seasonal and diurnal time scales, and covers all possible forcing scenarios. The data sets were taken from ocean sites in the North Pacific and North Atlantic and offer contrasting oceanographic conditions. For example, the LOTUS data chosen can be described as having a combination of weak winds and strong heating which is ideal for testing the proposed parameterization for z_0 since the z_{0fc} correction term becomes important. The OWS P data, on the other hand, can be generally described as having significantly stronger winds and weaker solar heating. The reason for including this data set is to demontrate that the term z_{0fc} becomes negligible under these conditions and the z_0 parameterization effectively reduces to the usual Charnock formula. We next present the results obtained from these simulations.

4.1. LOTUS DATA SET

LOTUS is an acronym which stands for Long-Term Upper-Ocean Study, and refers to a 2 year experiment which began in May 1982. It was conducted in the North Atlantic in the Sargasso Sea located at 34°N and 70°W (off the east coast of U.S.A. approximately 330 km from the mean path of the Gulf Stream). The main scientific goal of this experiment was to study the response of the upper ocean to a variety of atmospheric forcings, and environmental situations such as the presence of Gulf Stream rings. Details regarding the experiment, and results obtained have been reported in several studies including Briscoe and Weller [25], Cornillon and Stramma [26], Price *et al.* [27] and Stramma *et al.* [28] to list a few.

From this data set an 8 day period beginning on July 13, 1982, which we denote as day 0 in our simulations, was selected to test the sensitivity to the roughness length parameterization on time scales of several days. This particular period was chosen because relatively little advection was observed, thus making it well suited for a one-dimensional model. This same period was also used in several previous studies which include: Large *et al.* [29] and Kantha and Clayson [30]. The data set consists of surface meteorological measurements, as well as solar radiation taken regularly every 15 min. The surface meteorological data include wind speed and direction, air pressure and temperature, and SST. We point out that the SST recorded does not correspond to $z = 0$ but rather $z = -0.6$ m. Subsurface profiles of temperature and horizontal velocity components were also recorded at depths of 5, 10, 15, 20, 25, 35, 50, 65, 75 and 100 m. The computational parameters used in the numerical simulations were chosen to correspond closely with the measurements so as to minimize errors associated with interpolation. For example, the time step used was 15 min. which agrees with the sampling time. Also, a uniform grid spacing of 1 m down to a depth of 150 m was found to provide adequate resolution. Since the mean quantities are computed midway between the grid points (to allow for accurate differencing) the topmost computed temperature (i.e., SST) actually occurs at $z = -0.5$ m and agrees closely with the depth of the recorded SST. The observed profiles for $\overline{U}$, $\overline{V}$ and $\overline{\theta}$ were used as initial conditions in our simulations. Salinity was not recorded, and hence, was assumed to remain constant over the simulation period, as was the relative humidity which was fixed at 75%. As in Stramma *et al.* [28], the extinction of solar radiation was modelled according to Paulson and Simpson [31] assuming optical properties corresponding to water optical type I, where we have also assumed a 6% surface albedo.

We recognize that, in reality, the proper temperature to be used in computing the surface fluxes is the true surface temperature T_s at $z = 0$. As pointed out by Saunders [32] and Paulson and Simpson [33], T_s is typically a few tenths of a degree cooler than the temperature a few centimeters below due to the cool-skin effect. In addition, the warm-layer effect, caused by the solar radiation deposited in the upper few meters, should also be accounted for. Corrections for both of these effects can be handled using the method of Fairall *et al.* [39, 40]. The approach adopted in this study is to use the recorded temperaure at $z = -0.6$ m in computing the fluxes. The reason for this is that we are primarily interested in the impact of the z_0 parameterization on the SST, and by introducing corrections for the cool skin and warm layer this will mask the contribution brought on by the surface roughness parameteriztion. Thus, we have decided to use the recorded temperature and to compare simulated and observed temperatures at more or less the same depth.

The atmospheric forcing during this period is characterized by weak winds and strong heating, and is illustrated in Figures 1a–c. Figure 1a reveals that we are dealing with an 8 day stretch of essentially cloud-free weather, while Figure 1b shows that the winds are weak during this period. A consequence of this combination is that the SST underwent large-amplitude diurnal warming episodes as portrayed in Figure 1c. As previously mentioned, these are perfect conditions to test our new parameteriztion. Because of the weak winds, the results turned out to be insensitive to the initial conditions used for $\overline{U}$ and $\overline{V}$.

We begin by assessing the performance of the mixed-layer model over the simulation period by comparing the heat content. Plotted in Figure 2a is the observed and simulated heat content which corresponds to the LHS of Equation (38). The agreement between simulation and observation is good overall with noticeable differences occurring during days 5 and 6. This suggests that a one-dimensional mixed-layer model should be valid over that period. Further support of this is shown in Figure 2b which compares the simulated LHS and RHS of Equation (38). Clearly visible in Figure 2b is the modulating effect of the strong diurnal cycle.

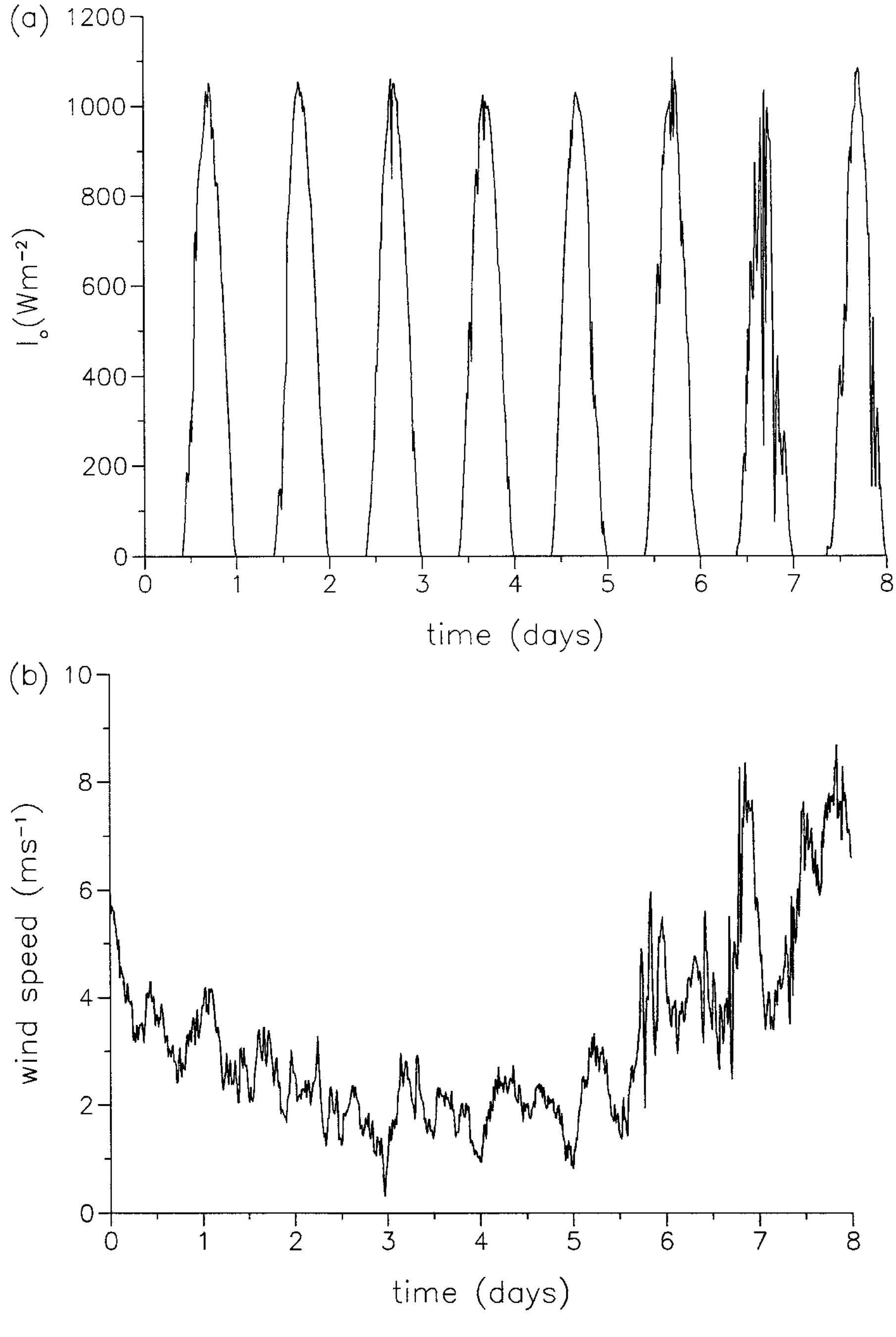

Figure 1. (a) Observed insolation recorded during LOTUS. (b) Observed winds recorded during LOTUS. (c) Observed SST recorded during LOTUS.

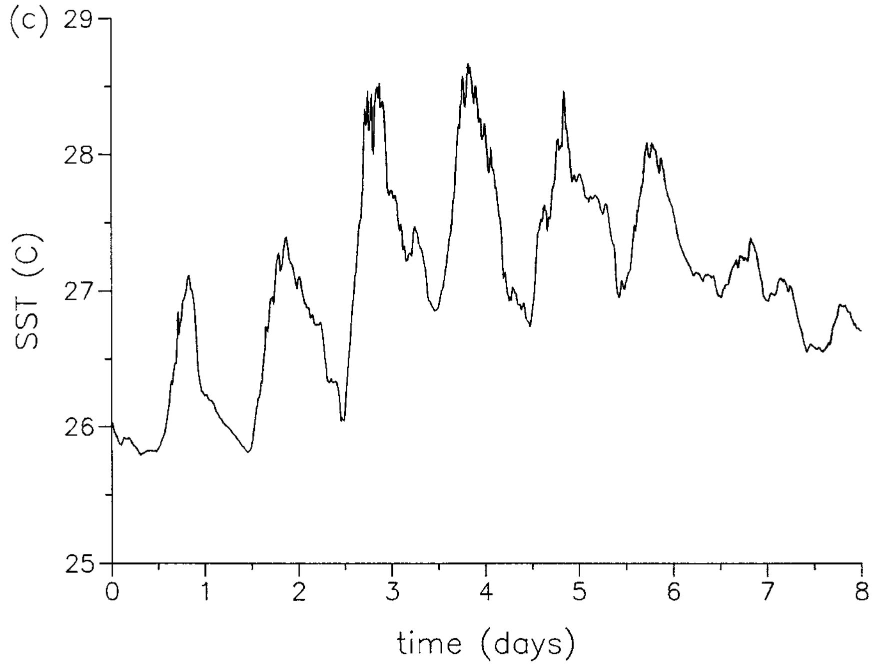

Figure 1. Continued.

Further discussion of diurnal dynamics in the oceanic mixed layer can be found in Noh [34]. In Figure 2a D was set to 15 m. The idea here was to select a depth close to the surface yet below the mixed layer since this vertical portion would be most influenced by surface forcing. Because of the weak winds observed, the effect of mixing will be minimal; the strong solar heating also established considerable stratification that further acted to suppress mixing. Consequently, a very shallow mixed layer resulted which allowed $D = 15$ m as a sufficient depth over which to check the changes in heat content. A larger depth, though, was used in Figure 2b to ensure that the fluxes at $z = -D$ become sufficiently small. This is a necessary condition in order for Equation (38) to hold.

Contrasted in Figure 3 are the simulated and observed SST using various roughness length parameterizations. The diagram reveals that the Smith [4] formulation behaves very similar to the Charnock formulation while the new parameterization proposed performs considerably different. In addition, the new parameterization results in a significant improvement in agreement between the observed and simulated SST. It is worth noting that all simulations drift away from observation and largely overestimate the SST during days 5 and 6. This interestingly coincides with the times that the heat balance was off and may provide an explanation for the departure in SST. Comparisons of the simulated and observed temperatures at depths of 5, 10 and 15 m were also carried out and it was noticed that these simulated temperatures showed little sensitivity to the parameterization of z_0 used. This is

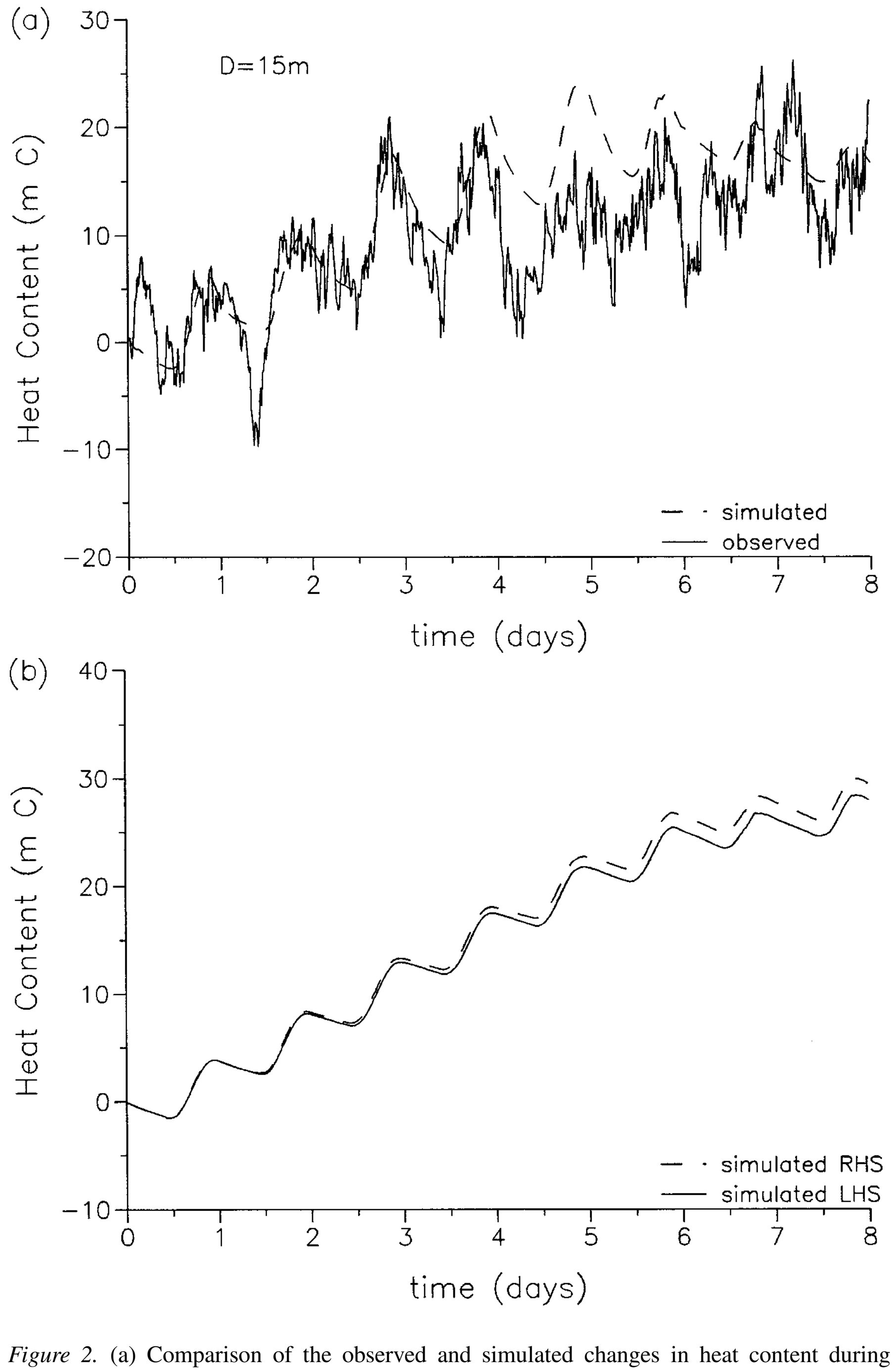

Figure 2. (a) Comparison of the observed and simulated changes in heat content during LOTUS. (b) Comparison of the simulated LHS and RHS of Equation (38) during LOTUS.

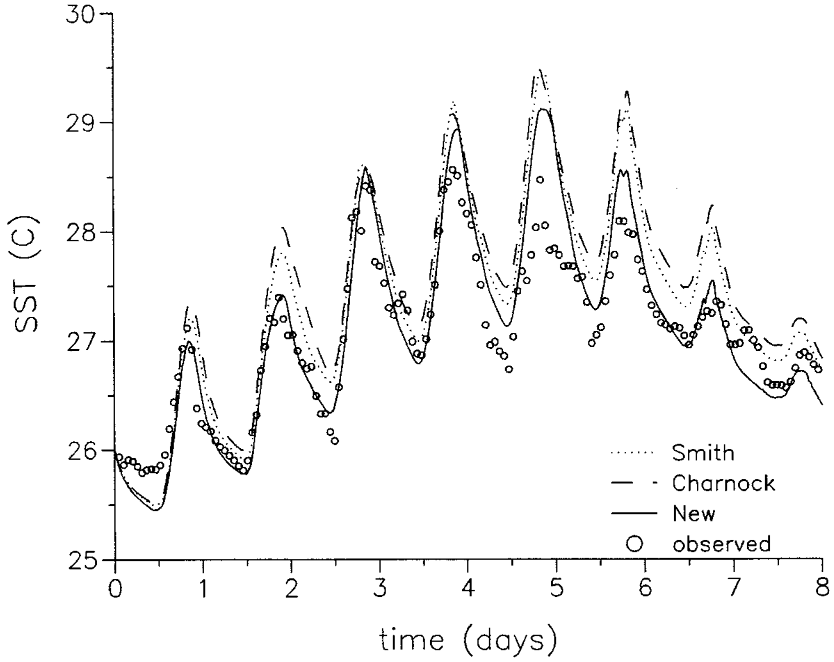

Figure 3. Comparison of the observed and simulated SST during LOTUS using the Charnock, Smith and new paramterization for z_0.

probably due to the strong stratification and little mixing which essentially damped out the z_0 influence. This suggests that the differences in simulated SST are due mainly to the differences in surface fluxes resulting from the different roughness length parameterizations and not due to mixing or effects of the deeper ocean.

The simulation conducted at LOTUS demonstrates that the computed SST shows noticeable sensitivity to the parameterization of z_0 as well as the ability of the mixed-layer model to reasonably reproduce the observed diurnal cycle. Successful modelling of the diurnal cycle is an essential ingredient in weather forecasting. We next examine the sensitivity on the longer seasonal cycle which is important in climate modelling. For this purpose we now turn our attention to the OWS P data set.

4.2. OCEAN WEATHERSHIP STATION PAPA DATA SET

The model sensitivity to surface forcing resulting from different roughness length paramterizations was further tested against observational data taken from OWS P located in the North Pacific at 50°N, 145°W (approximately 1,000 km from the northern tip of Vancouver Island). This corresponds to a location where ships would routinely go and take surface meteorological measurements as well as sub-surface profiles of temperature. With this data set a year-long simulation was carried out for the year 1961. This particular year was chosen for two main reasons.

Firstly, it represents a year where the data set is quite complete, and secondly, it corresponds to a year that other researchers such as Martin [35], Large, McWilliams and Doney [29] and Kantha and Clayson [30] have used to test other models, and therefore allows comparisons to be made with other models if necessary. In this simulation day 0 denotes January 1st, 1961. The model was run with an average 5 m grid spacing which extended down to a depth of 200 m, and a 15 min. time step. While other grid spacings were used, the overall agreement showed little dependence on the grid size. This is further discussed in D'Alessio *et al.* [5].

The data set consists of 3-hourly meteorological measurements, and temperature profiles. The observed temperature profile was used to initialize the temperature at the beginning of the simulation. From the meteorological data (which included SST, air, wet-bulb and dew point temperatures, wind speed and direction, cloud cover and surface air pressure) surface fluxes of heat, momentum, and evaporation were computed once again using the AM96 scheme. Fluxes required by the model between the 3-hourly measurements were obtained by linear interpolation. Initial profiles for the mean velocity components and salinity were not available from the data set. Salinity was specified according to the climatological data of Beatty [36]; this was justified in the work by D'Alessio *et al.* [5] by comparing runs using different methods of specifying the salinity profile. On the other hand, $\overline{U}$ and $\overline{V}$ were initially set to zero. Again, it was shown in D'Alessio *et al.* [5] that the simulations show little dependence on the initial $\overline{U}$ and $\overline{V}$ profiles. The extinction of solar radiation was modelled according to Paulson and Simpson [31] assuming optical properties corresponding to water optical type II, where we have also assumed a 6% surface albedo. Solar radiation was estimated using the Fritz formula for clear-sky insolation and was corrected for cloud cover according to Tabata [37]. Lastly, the precipitation was specified on the basis of the mean observed annual cycle of Tabata [38].

As before, we begin by presenting the changes in the vertically integrated heat content given by the LHS of Equation (38). Graphs of the observed and simulated heat content are shown in Figures 4a–c for the depths of 50, 100 and 200 m respectively. The observed heat content was averaged over 10 consecutive measurements so as to reduce the fluctuations. The graphs indicate reasonable agreement between observation and simulation and support the use of a one-dimensional mixed-layer model over the selected period. As D increases the agreement between observation and simulation worsens, probably owing to the contribution from the deeper ocean. As pointed out earlier there is no interaction between the mixed layer and the deeper ocean. This omission can cause significant errors to result. Ideally, D should be chosen to lie below the maximum mixed-layer depth which at OWS P is about 175 m. However, the maximum mixed-layer depth takes place during the wintertime, and thus, apart from the wintertime D can be taken to be much less than 175 m. By comparing Figures 4a–c we see that the largest discrepancy between simulation and observation takes place near the end of the simulation period. Since the mixed-layer depth is below 100 m during that interval, this reinforces our claim

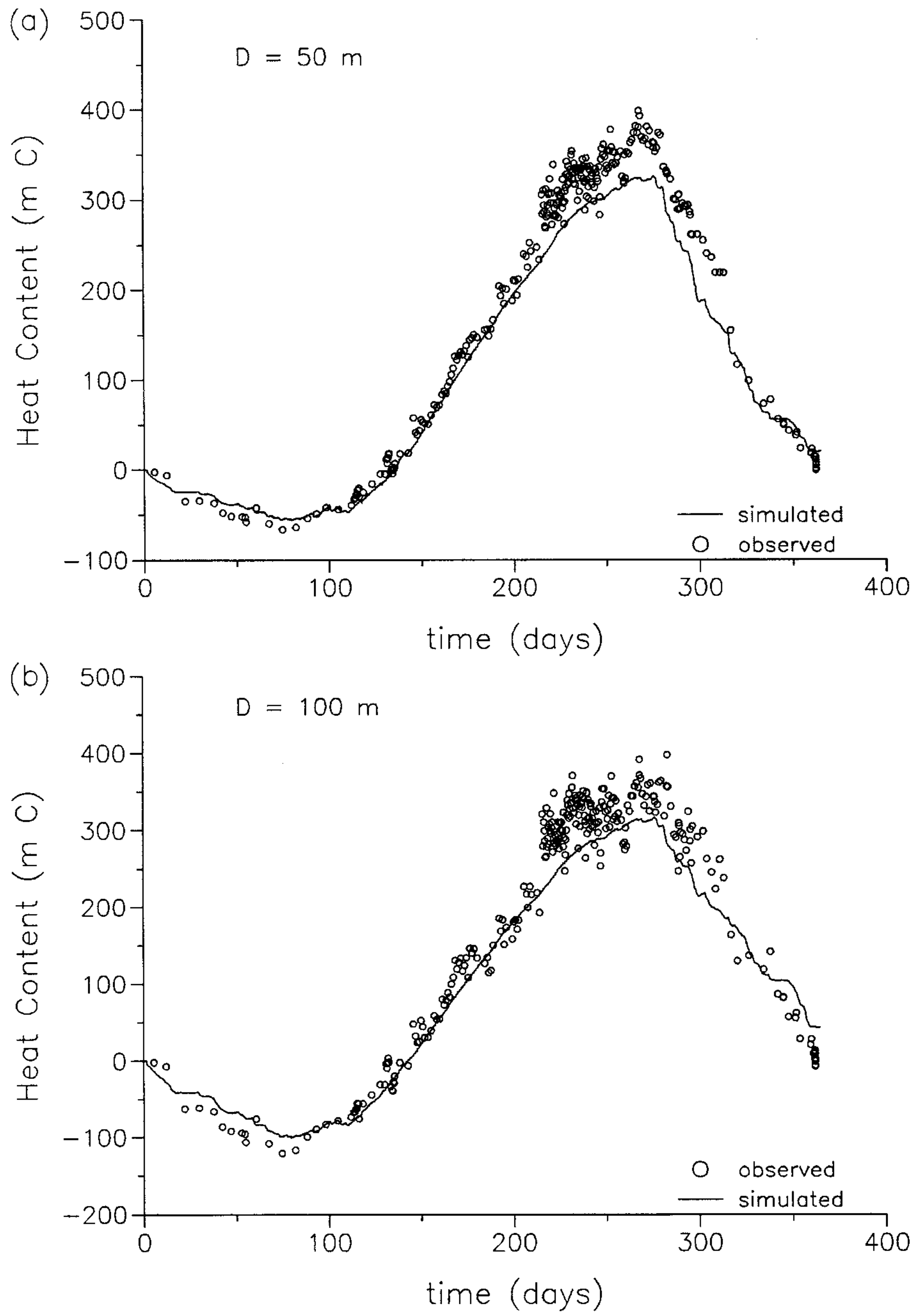

Figure 4. (a) Comparison of the observed and simulated changes in heat content at OWS P for $D = 50$ m. (b) Comparison of the observed and simulated changes in heat content at OWS P for $D = 100$ m. (c) Comparison of the observed and simulated changes in heat content at OWS P for $D = 200$ m.

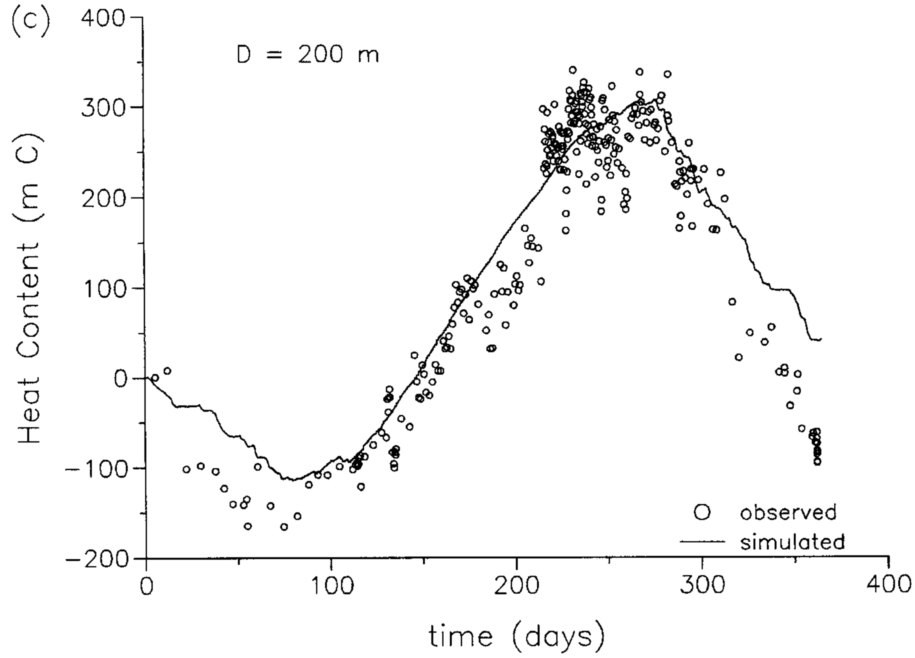

Figure 4. Continued.

that the effect of the deeper ocean does play a significant role in disrupting the heat balance.

In Figure 5 we compare the simulated and observed SST during this year-long simulation. Here, the simulated SST was computed using the new parameterization for z_0. The changes in SST caused by using the Charnock and Smith formulations of z_0 were of little consequence. This finding is not surprising though since the winds at OWS P were typically much stronger than those during the LOTUS simulation. Thus, the new formulation essentially reduces to a Charnock-type parameterization. It is important that the new parameterization behaves correctly in both limits: strong winds and weak winds/strong heating. Although only SST comparisons were presented here, temperature profiles at various instants in time also displayed little sensitivity to the roughness length parameterization. These simulated profiles agreed fairly well with the observed profiles of temperature except in the deeper ocean.

The agreement between the simulated and observed SST is consistently very good during the entire run. It is worth mentioning that in previous studies such as Martin [35], Large [29] and Kantha and Clayson [30] the final simulated SST overestimates the observed SST by as much as 1°C. This overestimation can be due in part to the different schemes used to compute the surface fluxes.

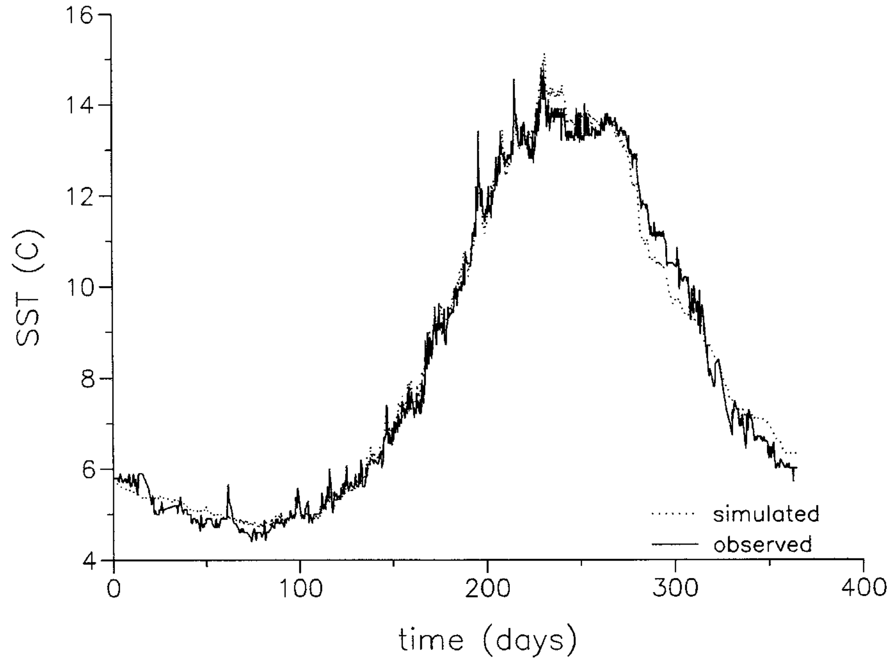

Figure 5. Comparison of the observed and simulated SST at OWS P for the year 1961 using the new parameterizations for z_0.

5. Conclusions

This paper presents a study of the response of the upper ocean to the parameterization of the atmospheric roughness length. This was investigated using the recently developed turbulence closure scheme of D'Alessio *et al.* [5] driven by the Abdella and McFarlane [6] surface flux scheme which is a non-iterative scheme and is currently used in the Canadian Center for Climate Modelling and Analysis GCM. Recognizing the difficulties of exisiting momentum roughness formulations in the free convection limit when both the wind speed and the friction velocity approach zero, a new formulation is proposed. The new formulation extends Charnock's formula down to zero friction velocity and removes the singularity of Smith's [4] formula by accounting for the surface roughness due to free convective transfers. The new formulation essentially reduces to the usual Charnock formula in scenarios of moderate to strong winds. The value of a parameter appearing in the new formulation is determined by making use of exsisting free convection surface flux parameterizations. The new formulation appears to improve the overall agreement between the observed and simulated sea-surface temperature especially in cases of weak winds. This is supported by observational data sets taken from OWS P and LOTUS. This is most visible from the simulation carried out with the LOTUS data since the period chosen is characterized by weak winds and strong heating and is therefore ideal for testing the proposed formulation of the roughness length. The longer simulation carried out at OWS P, on the other hand, shows little sensitivity. This is to be expected though since the winds are in general much stronger. Thus, the new scheme correctly approaches the usual Charnock formula under conditions of moderate to strong winds.

Further, the new parameterization can be easily extended to take the state of the sea and wave breaking into account, and can therefore be a useful and important parameterization for use in a coupled atmosphere-ocean model. Possible extensions of this work include developing parameterizations for the roughness lengths for heat and moisture. In this study we have assumed that $z_0 = z_q = z_t$.

Acknowledgments
KA and SJDD wish to acknowledge financial support provided by the Natural Sciences and Engineering Research Council of Canada. The authors also gratefully acknowledge Paul J. Martin of the Naval Research Lab for providing the OWS data for station P, and Konstantin Zahariev of the Canadian Centre for Climate Modelling and Analysis for providing the LOTUS data.

Appendix A: Description of the AM96 Surface Flux Scheme

The nondimensional stability functions ψ_m and ψ_h used in the AM96 scheme are the following flux-profile relationships proposed by Paulson [9] and Dyer [10] for unstable conditions $(L < 0)$

$$\psi_m = 2\ln\left(\frac{1+\overline{x}}{2}\right) + \ln\left(\frac{1+\overline{x}^2}{2}\right) - 2\tan^{-1}(\overline{x}) + \frac{\pi}{2},$$

$$\psi_h = \psi_q = 2\ln\left(\frac{1+\overline{x}^2}{2}\right),$$

where $\overline{x} = (1 - 16\xi)^{1/4}$ and $\xi = z_1/L$. For stable conditions they use the more recent flux-profile relationships proposed by Beljaars and Holtslag [11]

$$-\psi_m = a\xi + b\left(\xi - \frac{c}{d}\right)\exp(-d\xi) + \frac{bc}{d},$$

$$-\psi_h = -\psi_q = \left(1 + \frac{2}{3}a\xi\right)^{\frac{3}{2}} + b\left(\xi - \frac{c}{d}\right)\exp(-d\xi) + \frac{bc}{d} - 1,$$

where $a = 1.0$, $b = 0.667$, $c = 5$ and $d = 0.35$. In terms of the nondimensional length scale ξ the following relation holds:

$$\xi = \frac{Pr^{-1}{\Psi_m}^2}{\Psi_h} Ri_B, \tag{A1}$$

where

$$\Psi_m = \ln\left(\frac{z_1}{z_0}\right) - \psi_m\left(\frac{z_1}{L}\right) + \psi_m\left(\frac{z_0}{L}\right),$$

$$\Psi_h = \ln\left(\frac{z_1}{z_t}\right) - \psi_h\left(\frac{z_1}{L}\right) + \psi_h\left(\frac{z_t}{L}\right),$$

$$Ri_B = \frac{g z_1\left(\overline{\theta}_{v1} - \overline{\theta}_{v0}\right)}{T_0 \overline{U_1}^2} .$$

In principle, Equation (A1) can be solved for ξ numerically for a specified set of parameters z_0, z_1, z_t and Ri_B which can then be used to determine the surface fluxes.

In order to avoid the computational costs associated with the full iterative solution of Equation (A1), AM96 proposed the following noniterative approximations for ξ obtained by examining appropriate asymptotic limits

$$\xi = Ri_B A_1\left(1 + \frac{A_2}{1 - \sqrt{A_3} Ri_B}\right), \tag{A2}$$

for unstable conditions and

$$\xi = Ri_B\left(\frac{A_1 + S(Ri_B)Ri_B + A_5 {Ri_B}^2}{A_4 Ri_B + 1}\right), \tag{A3}$$

for stable conditions. Here,

$$A_1 = \frac{\left(\ln\left(\frac{z_1}{z_0}\right)\right)^2}{\left(\ln\left(\frac{z_1}{z_t}\right)\right)\mathrm{Pr}},\ \ A_2 = 1 + 5Ri_B \ln\left(\frac{z_t}{z_0}\right)\left(\frac{z_t}{z_0}\right)^{\frac{1}{4}},$$

$$A_3 = \frac{z_1}{\sqrt{z_0 z_t}},\ \ A_4 = \frac{10\ln\left(\frac{z_1}{z_0}\right)\left(1 - \frac{z_0}{z_1}\right)}{\mathrm{Pr}\ln\left(\frac{z_1}{z_0}\right)},\ \ A_5 = \frac{27A_4}{8\mathrm{Pr}^2},$$

and

$$S\left(Ri_B\right) = \frac{s_1 \mathrm{Pr}\left(\ln\left(\frac{z_1}{z_t}\right)\right)^{\frac{1}{2}} A_5}{2 - s_2 Ri_B exp\left(-s_3 Ri_B\right) + s_4 {Ri_B}^2},$$

with $s_1 = c/2 = 2.5$, $s_2 = bc/d - 1 = 8.53$, $s_3 = bc = 3.35$ and $s_4 = 0.05$. In the above it has been assumed that $z_q = z_t$.

To account for free convection conditions which occur over warm surfaces and weak winds AM96 redefined the mean wind $\overline{U_1}$ by

$$\overline{U}_{1f} = \sqrt{\overline{U_1}^2 + (\beta w_{*a})^2},$$

where the parameter β is of the order of unity and w_* is the free convection velocity scale given by

$$w_* = \left(\frac{g}{T_0} \overline{\theta_v' w'}_0 z_i \right)^{\frac{1}{3}},$$

where z_i is the height of the boundary layer. Therefore, in the free convection conditions the following relation results

$$u_* = \frac{k\beta w_*}{\Psi_m},$$

so that w_* essentially replaces the friction velocity u_*. AM96 tested this cost-effective noniterative flux formulation over a wide range of parameter values and showed that the formulation is quantitatively as well as qualitatively consistent with the fully iterated solution.

References

1. Beljaars, A.C.M.: 1994, The parametrization of surface fluxes in large-scale models under free convection, *Q.J.R. Meteorol. Soc.* **121**, 255–270.
2. Miller M. J., Beljaars, A.C.M. and Palmer, T.N.: 1992, The sensitivity of the ECMWF model to the parameterization of evaporation from tropical oceans, *J. Climate* **5**, 1013–1043.
3. Smith, S.D.: 1989, Water vapour flux at the sea surface, *Boundary-Layer Meteorol.* **47**, 277–293.
4. Smith, S.D.: 1988, Coefficients for sea surface wind stress, heat flux, and wind profiles as a function of wind speed and temperature, *J. Geophys. Res.* **93**, 15467–15472.
5. D'Alessio, S.J.D., Abdella, K. and McFarlane, N.A.: 1998, A new second-order turbulence closure scheme for modelling the oceanic mixed layer, *J. Phys. Oceanogr.* **28**, 1624–1641.
6. Abdella, K. and McFarlane, N.: 1996, Parameterization of the surface-layer exchange coefficients for atmospheric models, *Boundary-Layer Meteorol.* **80**, 223–248.
7. Monin, A.S. and Obukhov, A.M.: 1954, Basic laws of turbulent mixing in the atmosphere near the ground, *Akad. Nauk. S.S.S.R. Trud. Geofiz. Inst.* **24**, 163–187.
8. Businger, J. A., Wyngaard, J.C., Izumi, Y. and Bradley, E.F.: 1971, Flux profile relationship in the atmospheric surface layer, *J. Atmos. Sci.* **28**, 181–189.
9. Paulson, C.A.: 1970, The mathematical representation of wind speed and temperature profiles in the unstable atmospheric surface layer, *J. Appl. Meteorol.* **9**, 856–861.
10. Dyer, A.J.: 1974, A review of flux-profile relationships, *Boundary-Layer Meteorol.* **20**, 35–49.
11. Beljaars, A.C.M. and Holtslag, A.A.M.: 1991, Flux parameterizations over land surfaces for atmospheric models, *J. Appl. Meteorol.* **30**, 327–341.
12. Uno, I., Cai, X.M., Steyn, D.G. and Emori, S.: 1995, A simple extension of the Louis method for rough surface layer modelling, *Boundary-Layer Meteorol.* **76**, 395–409.
13. Charnock, H.: 1955, Wind stress on a water surface, *Q.J.R. Meteorol. Soc.* **81**, 639–640.
14. Charnock, H.: 1958, A note on empirical wind-wave formulae, *Q.J.R. Meteorol. Soc.* **84**, 443–447.
15. Garratt, J.R.: 1977, Review of drag coefficients over oceans and continents, *Mon. Wea. Rev.* **105**, 915–929.
16. Wu J.: 1980, Wind-stress coeeficients over sea surface near neutral conditions. A revisit, *J. Phys. Oceanogr.* **10**, 727–740.

17. Janssen, P.A.E.M.: 1989, Wave-induced stress and the drag of air flow over sea waves, *J. Phys. Oceanogr.* **19**, 745–754.
18. Smith, S.D. and Coauthors: 1992, Sea surface wind stress and drag coefficients: The HEXOS results, *Boundary-Layer Meteorol.* **60**, 109–142.
19. Monin, A. S. and Yaglom, A.M.: 1971, *Statisitcal Fluid Mechanics*, Vol. 1, 769 pp., MIT Press, Cambridge.
20. Sykes, R.I., Henn, D.S. and Lewellen, W.S.: 1993, Surface-layer description under free-convection conditions, *Q.J.R. Meteorol. Soc.* **119**, 409–421.
21. Smith, S.D. and Banke, E.G.: 1975, Variation of the sea surface drag coefficient with wind speed, *Q.J.R. Meteorol. Soc.* **101**, 665–673.
22. Craig, P.D., and Banner, M.L.: 1994, Modeling wave-enhanced turbulence in the ocean surface layer, *J. Phys. Oceanogr.* **24**, 2546–2559.
23. Mellor, G.L. and Yamada, T.: 1974, A hierarchy of turbulence closure models for planetary boundary layers, *J. Atmos. Sci.* **31**, 1791–1806.
24. Mellor, G.L. and Yamada, T.: 1982, Development of a turbulent closure model for geophysical fluid problems, *Rev. Geophys. Space Phys.* **20**, 851–875.
25. Briscoe, M.G. and Weller, R.A.: 1984, Preliminary results from the Long-Term Upper-Ocean Study (LOTUS), *Dyn. Atmos. Oceans* **8**, 243–265.
26. Cornillon, P. and Stramma, L.: 1985, The distribution of diurnal sea surface warming events in the Western Sargasso Sea, *J. Geophys. Res.* **90**, 11,811–11,815.
27. Price, J.F., Weller, R.A., Bowers, C.M. and Briscoe, M.G.: 1987, Diurnal response of sea surface temperature observed at the Long-Term Upper Ocean Study (34°N, 70°W) in the Sargasso Sea, *J. Geophys. Res.* **92**, 14480–14490.
28. Stramma, L., Cornillon, P., Weller, R.A., Price, J.F. and Briscoe, M.G.: 1986, Large diurnal sea surface temperature variability: Satellite and *in situ* measurements, *J. Phys. Oceanogr.* **16**, 827–837.
29. Large, W.G., McWilliams, J.C. and Doney, S.C.: 1994, Oceanic vertical mixing: A review and a model with a nonlocal boundary layer parameterization, *Rev. Geophys.* **32**, 363–403.
30. Kantha, L.H. and Clayson, C.A.: 1994, An improved mixed layer model for geophysical applications, *J. Geophys. Res.* **99**, 25235–25266.
31. Paulson, C.A. and Simpson, J.J.: 1977, Irradiance measurements in the upper ocean, *J. Phys. Oceanogr.* **7**, 952–956.
32. Saunders, P.M.: 1967, The temperature at the ocean-air interface, *J. Atmos. Sci.* **24**, 269–273.
33. Paulson, C.A. and Simpson, J.J.: 1981, The temperature difference across the cool skin of the ocean, *J. Geophys. Res.* **86**, 11044–11054.
34. Noh, Y.: 1996, Dynamics of diurnal thermocline formation in the oceanic mixed layer, *J. Phys. Oceanogr.* **26**, 2183–2195.
35. Martin, P.J.: 1985, Simulation of the mixed layer at OWS November and Papa with several models, *J. Geophys. Res.* **90**, 903–916.
36. Beatty, W.H.: 1977, *Variability of Oceanographic Conditions at Ocean Weather Stations in the North Atlantic and North Pacific Oceans*, NAVOCEANO Technical Note 3700-67-77, U.S. Naval Oceanographic Office, Washington, D.C., 100 pp.
37. Tabata, S.: 1964, Insolation in relation to cloud amount and sun's altitude. In: Y. Kozo (ed.), *Studies on oceanography*, pp. 202–210, University of Washington Press, Seattle, Washington.
38. Tabata, S.: 1965, Variability of oceanographic conditions at ocean station 'P' in the northeast Pacific Ocean, *Trans. Roy. Soc. Can.* Vol. III, Ser. IV, 367–418.
39. Fairall, C.W., Bradley, E.F., Godfrey, J.S., Wick, G.A., Edson, J.B. and Young, G.S.: 1996a, Cool-skin and warm-layer effects on sea surface temperature, *J. Geophys. Res.* **101**, 1295–1308.
40. Fairall, C.W., Bradley, E.F., Rogers, D.P., Edson, J.B. and Young, G.S.: 1996b, Bulk parameterization of air-sea fluxes for tropical ocean-global atmosphere coupled-ocean atmosphere response experiment, *J. Geophys. Res.* **101**, 3747–3764.